ELSEVIER

Journal of Photochemistry and Photobiology A: Chemistry 100 (1996) 109–118

Journal of PHOTOCHEMISTRY AND PHOTOBIOLOGY A:CHEMISTRY

Photoinitiated polymerization reactions: application of a new real-time FTIR system for following the rate of polymerization

G. Bradley *, R.S. Davidson, G.J. Howgate, C.G.J. Mouillat, P.J. Turner

The Chemical Laboratory, University of Kent, Canterbury CT2 7NH, UK

Received 24 May 1996; accepted 10 June 1996

Abstract

During the development of a technique whereby the progress of cure in a photoinitiated polymerization reaction can be monitored by IR spectroscopy, a Fourier transform IR (FTIR) microscope was adapted to enable curing to be carried out on the microscope stage. Preliminary results are reported illustrating the effectiveness of the development for the observation of polymerization in acrylate, dioxolane and polymerizable liquid crystal systems.

Keywords: Photoinitiated polymerization; Real-time FTIR system; Rate of polymerization

1. Introduction

In recent years, research in the field of photoinitiated polymerization reactions has employed increasingly sophisticated real-time techniques for monitoring the progress of cure. Laser nephelometry requires samples to be dissolved in a specific solvent, and the progress of the reaction is followed by the increase in turbidity as polymerization proceeds [1]. Photodifferential scanning calorimetry can be used to follow the reaction exotherm and to determine the total amount of heat released during a reaction [2]. The use of IR spectroscopy has proved very popular for achieving the real-time monitoring of cure. This approach has benefited greatly from the simplicity of application. The initial work by Decker and Moussa [3] used a simple modification of a dispersive IR spectrometer, and as a technique variant has yet to be supplanted in terms of sampling speed.

However, dispersive IR spectrometers suffer from certain disadvantages. Firstly, the sample is held vertically in the beam of the spectrometer and must therefore be either of high viscosity or enclosed to ensure it remains in the beam for the duration of the experiment. If solution cells are employed for the latter, the use of systems which give rise to cross-linked polymers is precluded since the polymer will weld the windows together. Secondly, by their very nature, dispersive spectrometers are restricted in their operation to analysis at one wavelength. This is a weak point if shifts in the spectral baseline or changes in phase occur during the experiment.

Fourier transform IR (FTIR) spectrometers offer the means to overcome these disadvantages, albeit perhaps at the sacrifice of sampling speed. This speed limitation is implicit within the nature of the FTIR technique. FT mathematics derive frequency distribution data from an interferogram. Thus restrictions centre around the available slew rate of the moving mirror in the Michelson interferometer as it scans and the sampling rate of the associated detector. However, a complete spectrum of information is collected by scanning an interferogram burst.

The burst is a symmetrical pulse of information. The narrower the collected burst, the less spectral resolution carried by the information. Hence requirements for spectral resolution determine the maximum sampling speed for any given interferometer/detector combination. A complete spectrum will always be collected, permitting the monitoring of several peaks, baseline analysis and assessment of phase changes.

FTIR also offers the potential for using many different sampling techniques, some of which permit the sample to be held horizontally. However, practitioners of FTIR spectroscopy will be aware of a potentially crippling limitation. The capacity of FT systems to sum information is the factor permitting spectra of exceptional signal to noise ratio to be achieved from sampling methods previously difficult to employ. Various reflection techniques come into this cate-

* Corresponding author.

1010-6030/96/$15.00 © 1996 Elsevier Science S.A. All rights reserved
PII S1010-6030(96)04428-0

gory. Yet, the multiple accumulation of spectra magnifies the sampling speed limitations for a data point to be acquired for following cure.

It is only by operating in a transmission mode, either direct transmission or reflection transmission, that the signal to noise ratio for a single scan of the interferometer is adequate to be used alone. Previous workers have used these modes [4,5]. Since, in most circumstances, the use of direct transmission requires the sample to be vertical in the sample compartment, one potential advantage of using FTIR is negated. The reflection transmission accessory employed [5] permits the examination of the sample in a sloping position (not horizontal, but not as difficult for sample preparation as a vertical position). Reflection transmission techniques, by virtue of the fact that the analytical IR beam passes through the sample twice, are restricted to half the sample thickness of direct transmission.

With the use of an FTIR microscope, direct transmission becomes useful. The microscope possesses a horizontal sample stage which therefore eliminates sample retention problems. Furthermore, there are benefits in the fact that the required sample size for an FTIR microscope is substantially smaller than for other FTIR sampling techniques.

In this paper, we present some preliminary results to illustrate the value of the new development. In the first system examined, a formulation based on 1,6-hexanediol diacrylate (HDDA) and an aromatic epoxy acrylate was used. Exposure of this formulation containing an initiator system to UV light leads to free radical polymerization of the acrylate group to give hard cross-linked films. However, the film properties and the maximum percentage conversion can be affected by the type of photoinitiator used, the temperature of cure and the presence of additives [6]. Of these additives, tertiary amines can play a major role in free radical curing, especially when type II photoinitiators are used. These photoinitiators in their triplet state react with tertiary amines to yield an α-aminoalkyl radical which acts as the initiator. Amines are also very important as they counteract oxygen inhibition. Although tertiary amines are not absolutely necessary for formulations containing type I photoinitiators, it has long been considered that adding such an amine to these formulations may have a beneficial effect by reducing oxygen inhibition [6].

The second system concerns the relatively fallow, yet potentially interesting, field of dioxolane-based photopolymer systems. The free radical polymerization of 2,2′-diphenyl-4-methylene-1,3-dioxolane was found to occur via ring opening and the quantitative elimination of benzophenone [7] as shown in Fig. 1.

Unfortunately, this reaction is too slow to be followed using real-time techniques. The 4-methylene-1,3-dioxolane moiety contains a vinyl ether group which is known to polymerize rapidly in the presence of photogenerated acids. It was decided to examine the photoinitiated cationic reaction of this compound in order to establish whether the reaction gives the same products as the free radical-initiated reaction.

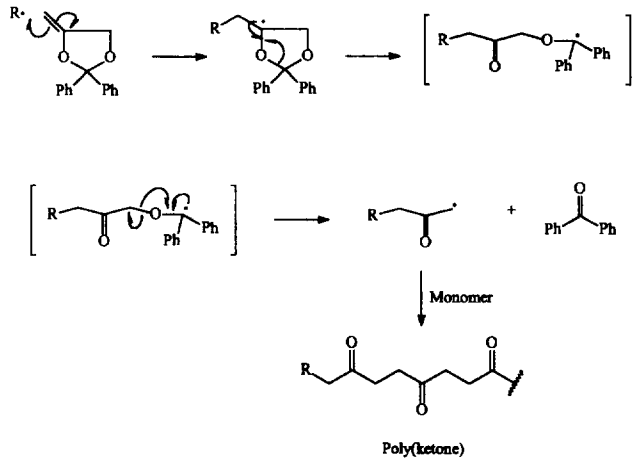

Fig. 1. Elimination of benzophenone during the radical polymerization of 2,2′-diphenyl-4-methylene-1,3-dioxolane.

In this case, the IR spectrum would be expected to show that the methylene group of 2,2′-diphenyl-4-methylene-1,3-dioxolane is consumed during the reaction. It would also be expected to show that this reaction leads to the generation of both dialkyl carbonyl and diaryl carbonyl groups. These three changes should be clearly visible by real-time FTIR, providing that the peaks do not overlap.

The third system describes the application of the new method for following the photoinitiated polymerization of acrylate liquid crystals. An important parameter which affects the rate of cure is the temperature. The properties of these materials also require their handling at elevated temperatures in order to obtain a working liquid and to acquire the correct liquid crystal phase. Thus a specially constructed heated microscope stage was used to investigate the rate of cure over a range of temperature. In the commercial environment, curing of these materials takes place in the presence of oxygen, and so samples were required to be open to the air.

2. Experimental details

2.1. Construction and modification of the instrument

The starting point for the operation was a Bio-Rad model FTS60 FTIR spectrometer (Cambridge, MA) fitted with a UMA-300A microscope complete with mercury cadmium telluride (MCT) detector. The microscope overview is shown in Fig. 2. Initial attempts to introduce UV light to the system used light guides. However, restrictions in the accessibility of the sample due to the short focal distance designed into the microscope objective curtailed this approach. A detailed examination of the microscope internal optics followed.

The UMA-300A microscope attachment permits interrogation of the sample both in transmission and reflectance (Fig. 3 and Fig. 4). As can be seen from Fig. 3 and Fig. 4, there is a bifurcation of the optical path part way through the light path. This bifurcation centres around a mirror which can

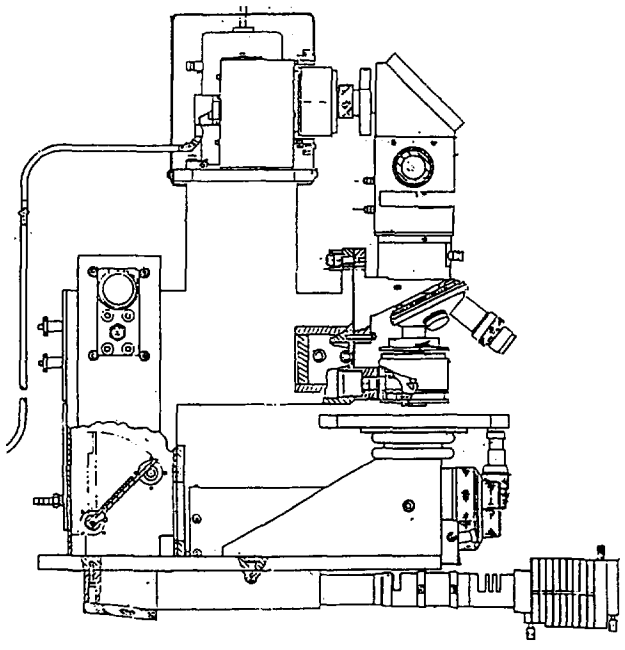

Fig. 2. Microscope attachment overview.

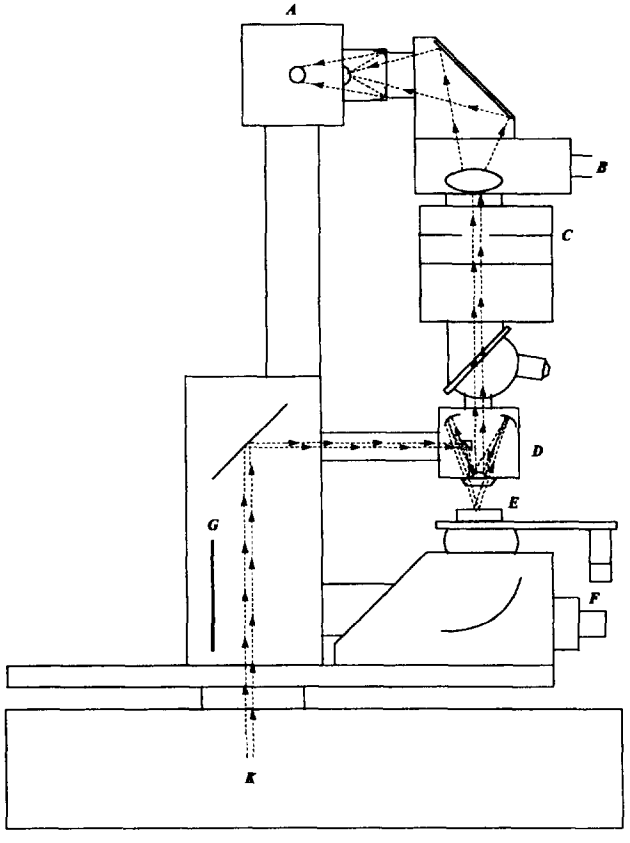

Fig. 3. Microscope reflection light path.

be pivoted into the beam to direct IR energy away from the reflection path and into the transmission path. It was noted that, when this mirror was set to direct light into the transmission path, the subsequent part of the reflection path was unused.

Design requirements specified aperture sharing in the microscope objective (Fig. 5). Thus, regardless of whether

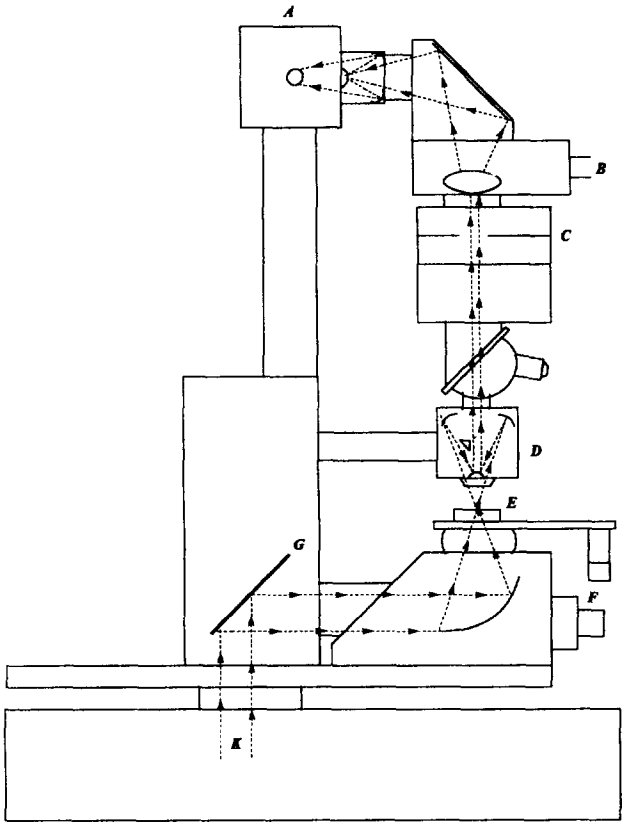

Fig. 4. Microscope transmission light path.

a sample was interrogated by transmission or reflection, the energy had to fall on the same area of the sample in order to be detected. The intriguing possibility of using the reflection light path to UV irradiate was considered. Close scrutiny of the involved optics showed that they consisted entirely of front silvered mirrors, suitable for UV as well as IR.

The addition of a further front silvered mirror on the reverse of the existing bifurcation mirror gave a light path for the UV which was easily accessible from outside the instrument (Fig. 6). In using this UV delivery system, the light had to be focused into the instrument. Light guides were therefore not applicable and a Kratos lamphouse with collimating optics was fitted. This arrangement resulted in the delivery of a concentrated 1 mm^2 area of light to the sample. Due to the restricted lifetime of short arc lamps, various lamps were used in the lamphouse for different applications.

To remove IR radiation from the UV source, a filter of deionized water in an aluminium housing with quartz windows was employed. The filter assembly was cooled using mains water delivered through a copper coil in contact with the aluminium housing (Fig. 6, H).

A simple gravity/magnetic release shutter was constructed for the lamphouse and placed between the lamp and the IR filter. This aluminium plate could be dropped from the beam when supply to the retaining electromagnet was cut (Fig. 6, I).

On the FTS60 instrument, a front panel light-emitting diode (LED) lights when the instrument begins sampling

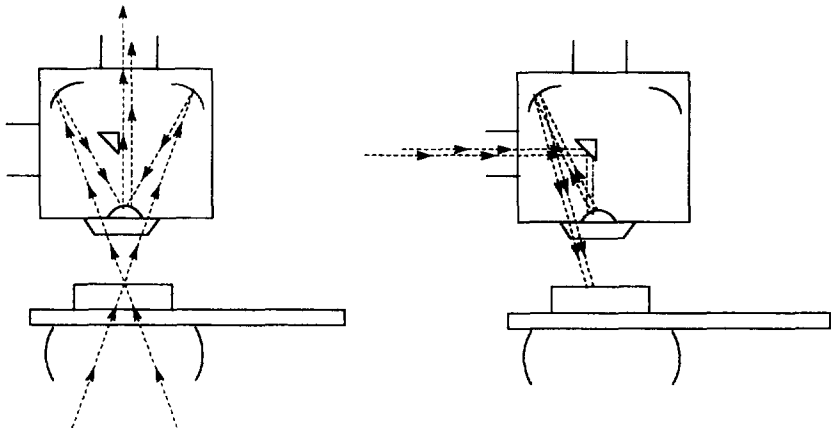

Fig. 5. Aperture sharing in microscope objective and its application to concurrent UV/IR irradiation.

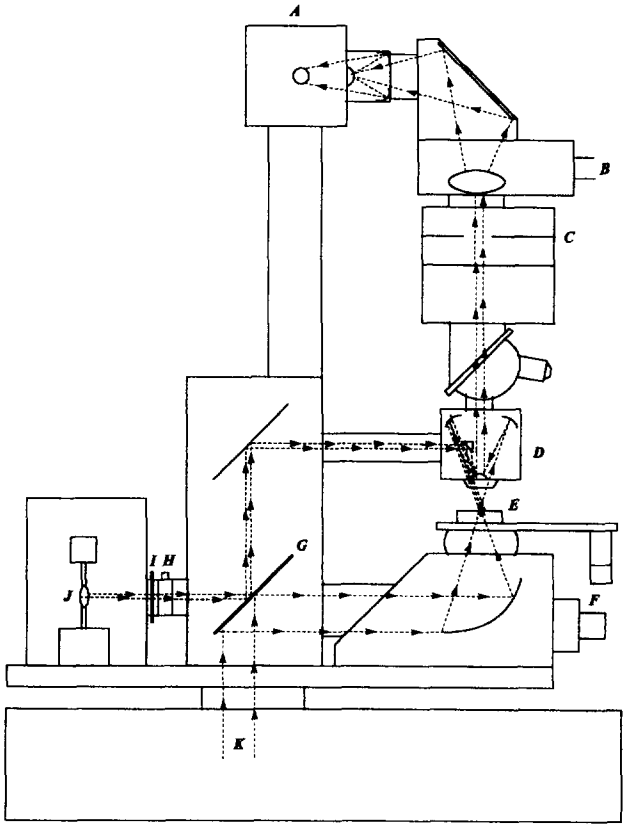

Fig. 6. Optical diagram of microscope and light source as used for concurrent irradiation: A, detector; B, viewfinder; C, aperture; D, lens; E, heated sample stage; F, focus control, stage movement; G, double-sided mirror; H, water-cooled IR filter to remove IR from UV lamp; I, mechanical shutter (opens when scanning starts to commence irradiation); J, UV source; K, IR spectrometer.

scans. The voltage applied to the LED was used as a trigger pulse to cut supply to the shutter electromagnet. Thus collect synchronization with UV irradiation was achieved.

2.2. Construction of sample handling accessory

For the initial work on the instrument, samples were simply coated or placed onto IR transparent plates and used on the microscope stage. Further development from this point involved the construction of a custom sample handling accessory in order to control the temperature and atmosphere under which cure occurs. Factors, such as the temperature at which curing takes place and the atmosphere prevailing over the sample, have a large effect on the cure and cure rate [8]. A stage module was thus constructed which permitted thermostatic control of the sample at temperatures ranging from room temperature to 150 °C, and allowed gas blanketing of the sample for atmosphere control.

A copper block was machined with a sample well, gold plated for corrosion resistance and enclosed in a Tufnol block for safety and insulation. At one end of the block, a heater was fitted, and the other end provided for either forced air or water cooling. A thermocouple was embedded in the copper adjacent to the sample. A duct machined in the copper allowed the sample well to be purged with gas for atmosphere control. A drawing is shown in Fig. 7.

The IR transmissive material used to form the base of the sample well was zinc selenide crystal, glued and clamped in place. Polytetrafluoroethene (PTFE) spacers were used to eliminate any stress applied to the crystal. The entire unit was secured in place of the normal slide carrier on the microscope stage. A three-term temperature controller (CAL 9900, R.S. Components) was used to permit accurate control and monitoring of the sample temperature.

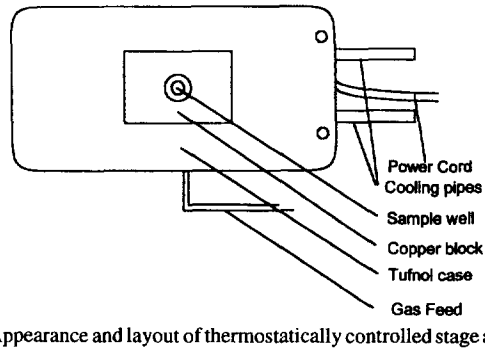

Fig. 7. Appearance and layout of thermostatically controlled stage accessory.

2.3. Experimental details for acrylate polymerization

2.3.1. Materials

HDDA (Aldrich), aromatic epoxy acrylate (Actilane 320TP20, Akcros), 2-benzyl-2-dimethylamino-1-(4-morpholinophenyl)-butanone-1 (Irgacure 369, Ciba Geigy), 2,2-dimethoxy-1,2-diphenylethan-1-one (Irgacure 651, Ciba Geigy), *N*-methyldiethanolamine (NMDE) (Aldrich) and ethyl-*p*-dimethylaminobenzoate (EPDMB) (Aldrich) were used as received.

2.3.2. Formulations

The formulations prepared for the experiment contained 5 wt.% of the desired amine when required and 2 wt.% of the photoinitiator in a 50/50 (wt./wt.) mixture of HDDA and the aromatic epoxy acrylate. The formulations were prepared in glass sample jars covered with black PVC tape in order to prevent polymerization during preparation and storage.

2.3.3. Preparation and curing of the sample

The real-time IR spectra were recorded using the modified Bio-Rad model FTS60 FTIR spectrometer fitted with a UMA-300A microscope complete with MCT detector described earlier. Using a pipette, a drop of the formulation was placed onto the zinc selenide crystal of the sample holder. The microscope was focused on the sample and the kinetic spectrum was collected and analysed using Bio-Rad Win-IR software. Spectra were collected at a resolution of 8 cm^{-1}.

Cure was followed by observing the acrylate absorbance at 810 cm^{-1}. When data collection had been completed and the three-dimensional spectrum of the curing of the formulation had been obtained, the data at 810 cm^{-1} were extracted using Bio-Rad Win-IR software and a plot of absorption vs. time was obtained. This plot was transformed using Microcal Origin software into a percentage conversion vs. time graph. The percentage conversion can be expressed as shown in Eq. (1)

$$\text{Conversion } (\%) = \frac{A_0 - A_t}{A_0} \times 100 \quad (1)$$

where A_0 is the absorbance of the 810 cm^{-1} peak before irradiation and A_t is the absorbance of the 810 cm^{-1} peak at a time t.

2.4. Experimental details for dioxolane work

2.4.1. Materials

2.4.1.1. 2,2'-Diphenyl-4-methylene-1,3-dioxolane synthesis

Step 1: ketalization

3-Chloro-propan-1,2-diol (50.0 g, 0.45 mol) was placed in a three-necked, round-bottomed flask (500 ml), together with benzophenone (18.2 g, 0.45 mol), benzene (300 ml) and 4-toluenesulphonic acid (0.2 g, 1.6 mmol). A Dean and Stark apparatus was set up and the solution was brought to reflux. The solution was then left to reflux for 24 h. After cooling, the benzene solution was extracted with a dilute aqueous sodium hydrogen carbonate solution followed by water. The organic layer was dried with anhydrous magnesium sulphate; after removal of benzene on a rotary evaporator, 2,2'-diphenyl-4-chloromethyl-1,3-dioxolane was distilled under reduced pressure (boiling point (b.p.) 150 °C at 200 mTorr). Yield, 18.4 g (67%).

IR spectrum (neat film): 1084, 1028 cm^{-1} (C–O–C), 754 cm^{-1} ($-C_6H_5$). ^1H NMR spectrum (100 MHz, $CDCl_3$, tetramethylsilane (TMS) reference): 7.3 ppm (multiplet, 10 H, $-C_6H_5$), 4.3 ppm (multiplet, 1 H, C–CH(–O)($-CH_2Cl$)), 4.0 ppm (multiplet, 2 H, O–CH_2–CH), 3.5 ppm (multiplet, 2 H, $-CH_2Cl$). Elemental analysis: expected: C, 69.9%; H, 5.5%; found: C, 69.9%; H, 5.5%.

Step 2: elimination

Potassium t-butoxide (22.0 g, 0.2 mol) was placed in a three-necked, round-bottomed flask (300 ml) with dry tetrahydrofuran (THF) (50 ml); a dropping funnel and condenser were fitted. The solution was stirred magnetically and heated to 55 °C. 2,2'-Diphenyl-4-chloromethyl-1,3-dioxolane (29.0 g, 0.1 mol) in dry THF (100 ml) was added dropwise over a period of 1.5 h, and the mixture was left for 5 h. The solution was then slowly added to distilled water (approximately 500 ml) and the product was extracted with diethyl ether. The ether was removed and 2,2'-diphenyl-4-methylene-1,3-dioxolane was distilled under reduced pressure (b.p. 120 °C at 300 mTorr). Yield, 19.5 g (82%).

IR spectrum (neat film): 1688 cm^{-1} (C=C), 1078, 1026 cm^{-1} (C–O–C), 748 cm^{-1} ($-C_6H_5$). ^1H NMR spectrum (270 MHz, $CDCl_3$, TMS reference): 7.4 ppm (multiplet, 10 H, $-C_6H_5$), 4.5 ppm (multiplet, 2 H, O–CH_2–C(–)=), 3.9 ppm (multiplet, 2 H, –C=CH). Elemental analysis: expected: C, 80.6%; H, 5.9%; found: C, 80.3%; H, 5.9%.

2.4.1.2. Other materials

[4-(Phenylthio)phenyl]diphenyl sulphonium hexafluorophosphate (Sericol) was used as supplied. The solvent employed in the formulation was γ-butyrolactone (Aldrich), which was also used as supplied.

2.4.2. Formulation

A solution was prepared in dark viols with 1 mol.% of [4-(phenylthio)phenyl]diphenyl sulphonium hexafluorophosphate in several drops of γ-butyrolactone and 99 mol.% of the dioxolane.

2.4.3. Preparation and curing

In this instance, a sodium chloride plate was used as sample support, the sample being placed dropwise onto the support.

2.5. Experimental details for liquid crystal work

2.5.1. Materials

Samples of acrylated liquid crystals, monoacrylated (M) and diacrylated (D), were kindly supplied by Merck. Irgacure 651 (Ciba Geigy) and Darocure 1173 were used as initiators.

2.5.2. Formulations

Photoinitiators were used at a level of 1%. These and the appropriate liquid crystal monomers were weighed into opaque 7 cm^3 vials using an analytical balance. In order to obtain a homogeneous mixture of the compounds, they were placed in a mechanical shaker for approximately 5 min and then immersed into boiling water until the mixture had melted. The melt was then thoroughly mixed by stirring.

2.5.3. Preparation and curing of the sample

Following this, the mixture was placed onto the thermostatically controlled zinc selenide crystal. Due to the exceptionally short pot life (perhaps thermal cure) of the molten liquid crystal materials, it is important that the scans are recorded as promptly as possible after the mixture has been prepared. As the irradiation spot is substantially smaller then the available sample area, it is possible to carry out many experiments quickly with each sample. This enables rapid temperature adjustment. The acrylate peak at 810 cm^{-1} was selected to indicate the concentration of remaining free acrylate. Analysis of the data was carried out as outlined in Section 2.3.3.

3. Results and discussion

3.1. Acrylate formulations

The graph obtained for the curing of the formulation containing Irgacure 369 and no amine (Fig. 8) gives some very important results. It can be seen that the rate of cure at the

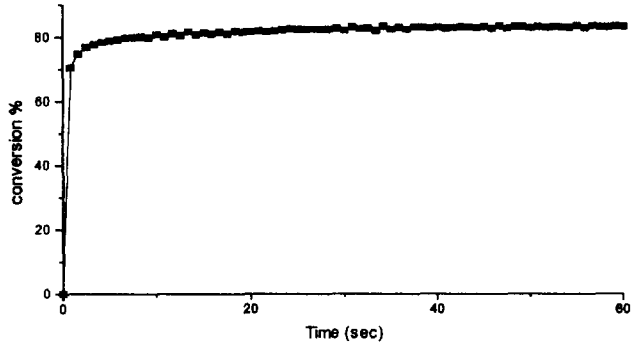

Fig. 8. Percentage conversion of the Irgacure 369 formulation without amine as a function of time.

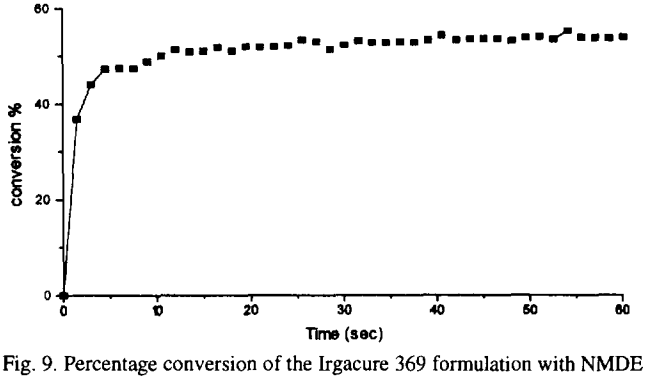

Fig. 9. Percentage conversion of the Irgacure 369 formulation with NMDE as a function of time.

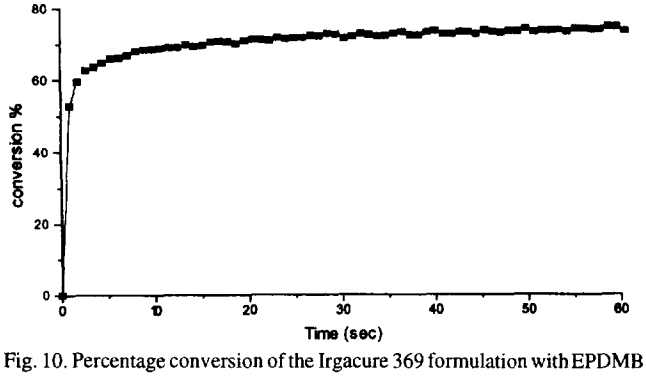

Fig. 10. Percentage conversion of the Irgacure 369 formulation with EPDMB as a function of time.

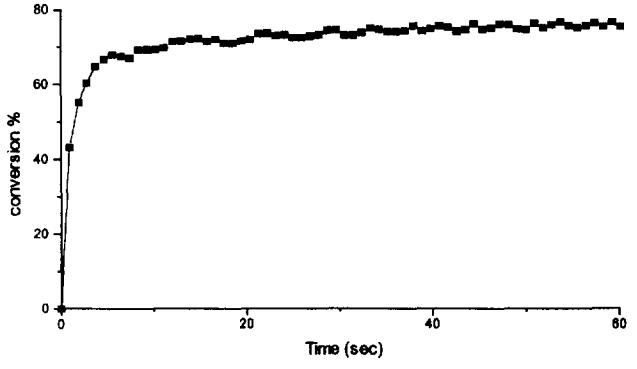

Fig. 11. Percentage conversion of the Irgacure 651 formulation without amine as a function of time.

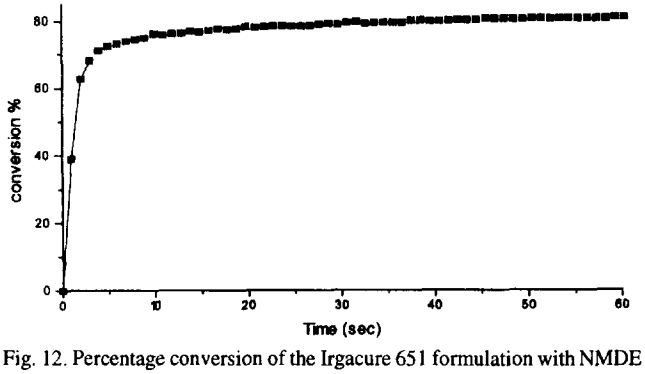

Fig. 12. Percentage conversion of the Irgacure 651 formulation with NMDE as a function of time.

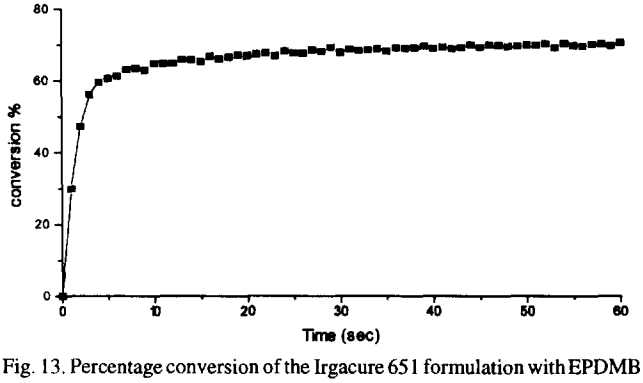

Fig. 13. Percentage conversion of the Irgacure 651 formulation with EPDMB as a function of time.

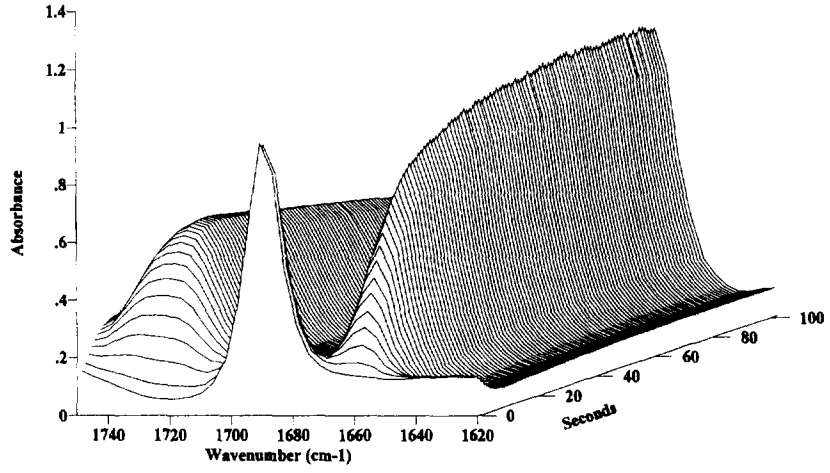

Fig. 14. Disappearance of vinyl and appearance of two carbonyl peaks during the cationic photopolymerization of 2,2′-diphenyl-4-methylene-1,3-dioxolane.

beginning of the exposure is very fast and, indeed, the formulation reaches 70% conversion after only 1 s. The maximum percentage conversion is 82% obtained after only 10 s.

When NMDE is added to the formulation, the graph obtained is quite different (Fig. 9). This time, the initial rate of cure is slower and, after 1 s, the percentage conversion is 30%. The maximum percentage conversion drops to 54% reached within roughly 25 s.

EPDMB seems to have a different effect on the curing of the formulation, and the plot of the percentage conversion vs. time (Fig. 10) once again has different characteristics. A conversion of 53% is reached after 1 s irradiation, and it takes 15 s to reach the maximum percentage conversion of 72%.

The effect of amines on the curing of a formulation containing type I photoinitiators was examined with a second photoinitiator: Irgacure 651. The graph obtained for the formulation without amine once again serves as a reference (Fig. 11). After 1 s, a percentage conversion of about 40% is reached. After 20 s, the maximum percentage conversion (75%) is obtained.

The Irgacure 651 formulation containing NMDE appears to cure in a very similar way (Fig. 12). A conversion of 40% is reached after 1 s and the maximum percentage conversion is reached after 20 s. The major difference separating the curing of these two formulations is the fact that the NMDE-containing formulation reaches a maximum percentage conversion of 80%.

The graph (Fig. 13) obtained for the formulation containing Irgacure 651 and EPDMB is slightly different. Once again, the maximum percentage conversion is obtained after 20 s irradiation, but this time it only reaches 70%. The percentage conversion after 1 s is 30%.

The addition of both NMDE and EPDMB to the Irgacure 369 formulation has a negative effect. This effect is characterized by a decrease in the maximum percentage conversion from 82% to 54% for the aliphatic amine and 72% for the

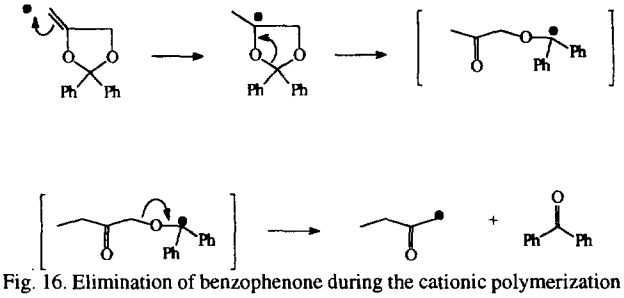

Fig. 16. Elimination of benzophenone during the cationic polymerization of 2,2′-diphenyl-4-methylene-1,3-dioxolane.

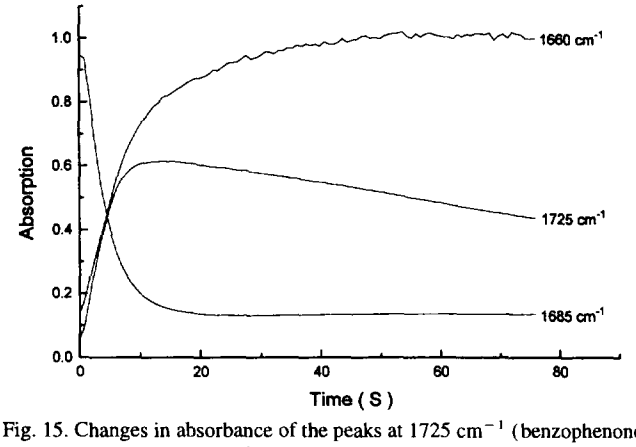

Fig. 15. Changes in absorbance of the peaks at 1725 cm^{-1} (benzophenone carbonyl group), 1685 cm^{-1} (vinyl group) and 1660 cm^{-1} (polymer carbonyl group) with time during the cationic photopolymerization of 2,2′-diphenyl-4-methylene-1,3-dioxolane.

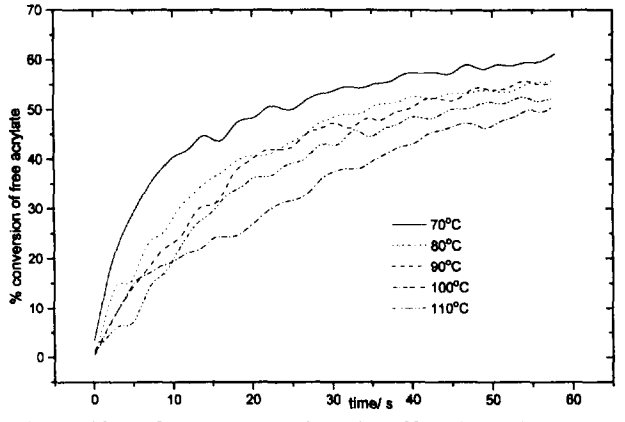

Fig. 17. Effect of temperature on the curing of Merck liquid crystal D.

aromatic amine. The initial rate of cure also decreases more for the aliphatic amine than for the aromatic amine. The addition of an aromatic amine, with its extensive UV absorption, may have a negative effect by absorbing light which would otherwise be available to the photoinitiator. This decrease in the amount of light available will lead to a decrease in the rate at which the initiator produces the initiating radical and, consequently, a decrease in the rate of cure. However, if this were solely the case, the effect of the aliphatic amine, which exhibits far less UV absorption, would be expected to be less. This is not the case. Another factor must contribute. Type II initiators based on aromatic carbonyls operate by hydrogen abstraction. This process takes place by electron transfer from an exciplex. It is feasible that, in the presence of such an exciplex-forming amine, operation via a type II mechanism may be forced. Type II operation from an initiator designed to operate as type I may result in the reduced efficiency observed.

The results obtained for the Irgacure 651 formulation are slightly different. As before, the addition of EPDMB has a negative effect on the maximum percentage conversion which drops slightly from 75% to 70%. The rate of cure also decreases. This is not seen for NMDE. The negative effect may be explained simply by the UV shielding exhibited by aromatic amines.

The most important point in this study is the observation that the addition of NMDE to the Irgacure 651 formulation has a beneficial effect, the maximum percentage conversion

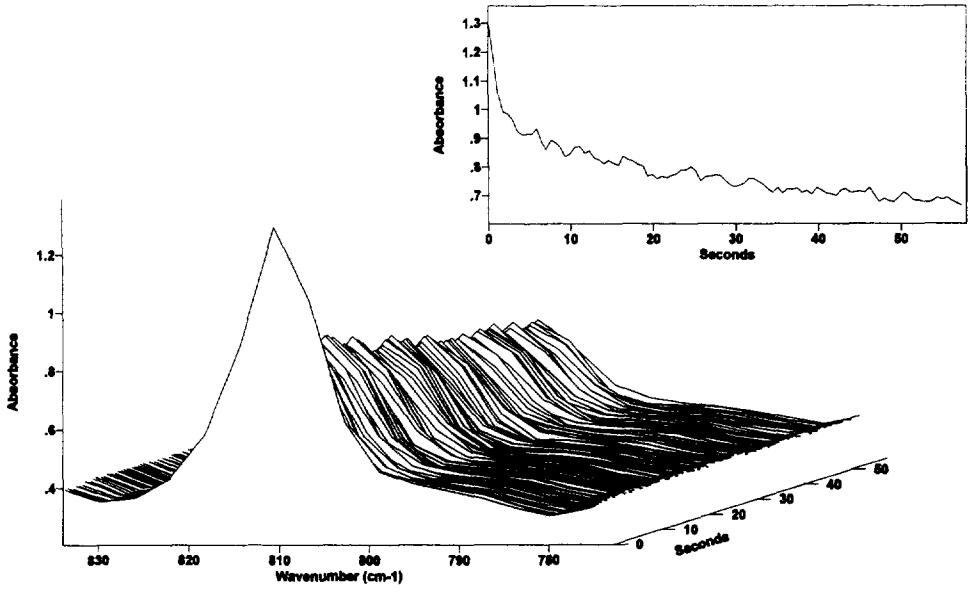

Fig. 18. Curing of Merck liquid crystal D using Irgacure 651 as initiator.

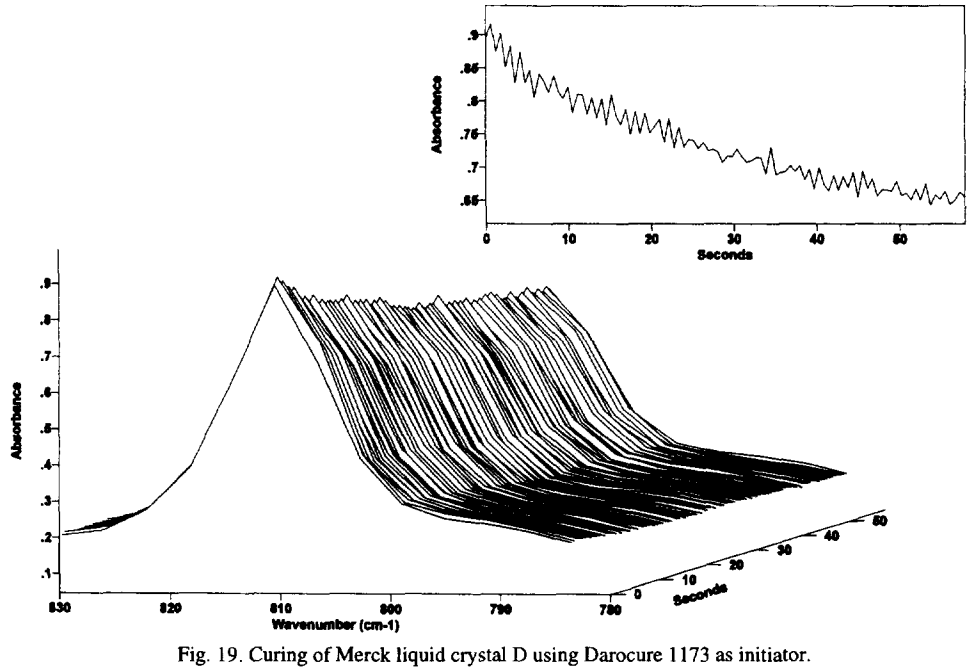

Fig. 19. Curing of Merck liquid crystal D using Darocure 1173 as initiator.

increasing from 75% to 80%. The initial rate of cure does not seem to be affected significantly. The increase in conversion observed for the Irgacure 651 formulation is probably due to the amine acting to restrict oxygen inhibition. Irgacure 651 produces radicals at a relatively slow rate and therefore is more vulnerable to oxygen inhibition, thereby reducing the maximum conversion. This increase in conversion obtained by the addition of an aliphatic amine has already been noted by Arsu et al. [8].

3.2. Results from dioxolane work

Some of the spectra obtained from real-time FTIR are shown in Fig. 14, which demonstrates that it is relatively easy to monitor the loss of a vinyl group (1685 cm^{-1}) and the build up of the polymer carbonyl group (1660 cm^{-1}) and benzophenone carbonyl absorption (1725 cm^{-1}). The three kinetics traces extracted from the spectra are shown in Fig. 15.

It is evident that the polymerization almost reaches completion, i.e. there is very little residual vinyl ether moiety after approximately 20 s of UV irradiation. This reflects in part the fact that the cured material is a liquid rather than a solid.

The changes in the three monitored peaks correspond to those expected from a free radical mechanism. Thus a similar route can be postulated for the cationic mechanism used here (Fig. 16).

3.3. Results from liquid crystal experiments

Initial studies were with the diacrylate (D). This has a nematic phase range of 77–127 °C, and polymerization experiments were carried out within this range. The use of a diacrylate presents problems due to cross-linking. During the formation of a cross-linked network, all the molecules are rigidly set in place before the reaction is complete. This means that complete polymerization cannot take place and acrylate groups are left unreacted in the finished product.

These experiments suggest that the rate of cure is greatest with a lower temperature (Fig. 17), and that Irgacure 651 is the most efficient photoinitiator (Fig. 18 and Fig. 19). The inverse relationship between the temperature and rate of cure may be due to the monomer units being aligned in a more ordered manner at lower temperatures such that they can react more readily.

When the lamp was changed from a high pressure mercury/xenon bulb to a high pressure mercury bulb, it was found necessary to filter the light because of the extra far-UV produced by the mercury lamp. Removal of the higher energy part of the UV was performed by placing a piece of Wood's glass in the beam. (The transmission characteristics of Wood's glass are shown in Fig. 20).

Real-time IR studies of the photopolymerization of the monoacrylate (M) did not give many satisfactory results.

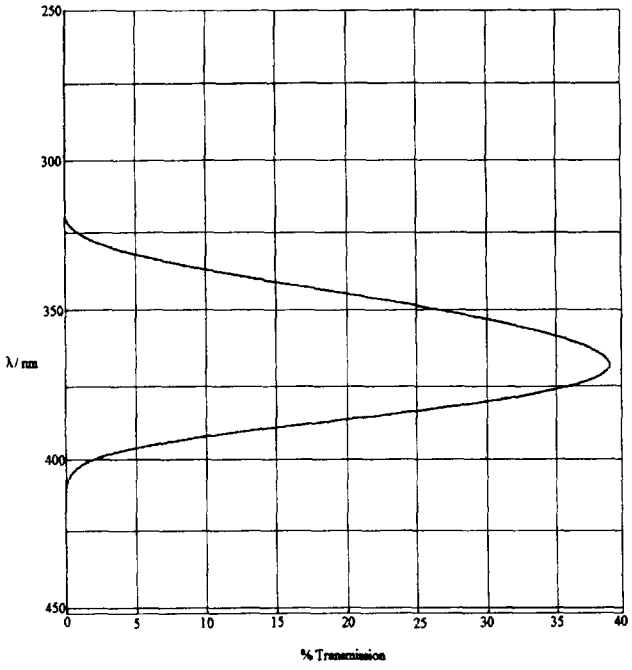

Fig. 20. Absorption characteristics of Wood's glass.

4. Conclusions

Real-time FTIR offers a reasonably clear view of polymerization processes. Even at cure speeds approaching the instrumental limitations, reliable data can be obtained. The maximum extent of cure is also easily obtained from these data. In industrial situations, this information can be used to fine tune exposure times to the required degree of cure.

This technique is also very useful in that it does not require a large amount of formulation. The results are quickly and very easily obtained. Even cross-linking systems can be easily worked with. Although a large area of cross-linked polymer is difficult to remove from the surface of an IR transmissive window, the very small piece of polymer formed by this technique can be easily removed from any surface.

Acknowledgements

We wish to thank Merck Ltd. (P.J.T.), Kobe Steel Ltd. (C.G.J.M.), Sericol Ltd. (G.J.H.) and the DTI ETIS initiative (G.B.) for financial support.

References

[1] C. Decker and M. Fizet, *Makromol. Chem. Rapid Commun., 1* (1980) 637.

[2] J.N. Leckenby, *Electronic Manufacturing, 19* (1988). G. Gozzelino, A. Priola and M. Mantegna, *J. Appl. Polym. Sci., 44* (1992) 927. J.L. Mateo, P. Bosch, F. Catalina and R. Sastre, *J. Polym. Sci., Polym. Chem., 30* (1992) 829. D.L. Kurdikar and N.A. Peppas, *Polymer, 35* (1994) 1004.

[3] C. Decker and K. Moussa, *Makromol. Chem., 189* (1988) 2381.

[4] A. Udagawa, F. Sakurai and T. Takahishi, *J. Appl. Polym. Sci., 42* (1991) 1861.
[5] D.B. Yang, *J. Polym. Sci., Polym. Chem., 31* (1993) 199.
[6] R.S. Davidson, in J.P. Fouassier and J.F. Rabek (eds.), *Radiation Curing in Polymer Science and Technology*, Vol. III, Elsevier, Barking, Essex, 1993, p. 153.
[7] Y. Hiraguri and T.J. Endo, *J. Am. Chem. Soc., 109* (1987) 3779. Y. Hiraguri and T.J. Endo, *J. Polym. Sci., Polym. Chem., 27* (1989) 2135. Y. Hiraguri and T.J. Endo, *J. Polym. Sci., Polym. Chem., 27* (1989) 4403.
[8] N. Arsu, R.S. Davidson and R. Holman, *J. Photochem. Photobiol. A: Chem., 87* (1995) 169.